Iranian Journal of Science and Technology, Transactions of Mechanical Engineering (2021) 45:321–336
https://doi.org/10.1007/s40997-019-00330-y

RESEARCH PAPER

Research on Dynamics Modeling and Simulation of Constrained Metamorphic Mechanisms

Yanyan Song[1,2] · Boyan Chang[1,2] · Guoguang Jin[1,2] · Zhan Wei[1,2] · Bo Li[1,2] · Yongjie Zhu[1,2]

Received: 6 September 2018 / Accepted: 30 October 2019 / Published online: 2 December 2019

Abstract
This paper presents a method for establishing a unified dynamics model of constrained metamorphic mechanisms. Based on the equivalent resistance, the influences of geometric constraints and/or force constraints on metamorphism are discussed, and the kinematic characteristics of metamorphic joints are described and analyzed in detail. On this basis, the metamorphic configurations of augmented Assur groups can be classified into three types, including non-collision, internal collision and external collision configurations, and the configuration complete dynamics models of augmented Assur groups are established. Then, the dynamics models of active parts, Assur groups and augmented Assur groups are summarized into a unified mathematical framework, and the unified dynamics model of constrained metamorphic mechanisms can be obtained. Based on the research mentioned above, the initial conditions of all components and the motion law of the active parts are given. The motion laws of all components, the driving force/torque of the active parts and the constraint force/torque of the metamorphic joints can be obtained by iteration and solution based on the theory that velocity and acceleration are same in an extremely brief period. Taking the planar double-folded metamorphic mechanism and the metamorphic nipper swing mechanism as examples, the computer numerical analysis and dynamic simulation are carried out to verify the correctness and effectiveness of the proposed theory and method.

Keywords Constrained metamorphic mechanisms · Augmented Assur groups · Dynamics · Iterative algorithm

1 Introduction

The metamorphic mechanisms originated from the study of foldable and erectable artifacts cartons (Dai and Rees 1997a, b, c) and were first proposed in 1998 at the 25th ASME Biennial Conference (Dai and Rees 1999). This kind of mechanism has the facilities to change configuration from one to another to fulfill the different function demands according to the changes in environment and working conditions (Ding and Yang 2010). In contrast to the traditional mechanism, metamorphic mechanisms have the innate ability to change their form, topology and configuration, from one type to another with resultant changes in the number of effective links, and the mobility of the mechanism in order to accomplish different tasks (Valsamos et al. 2012). This can be achieved by two approaches. One is to change the number of links by changing the coupled links and the linkage relationships (Liu and Yang 2004). The other is to apply constraint to joints to change the joint property. Parise et al. (2000) developed ortho-planar metamorphic mechanisms which can change their topological structures in two orthogonal planes and obtain the configuration change by reducing or increasing the number of effective links during operation. Zhang and Ding (2012) analyzed the constraint variation in the metamorphic mechanisms based on its multi-configuration characteristic and proposed a methodology for configuration syntheses in accordance with the realization of variation and coupling of adjacent configurations by applying metamorphic kinematic joints. Yan and Kuo (2006, 2007) investigated variable topology mechanisms and kinematic pairs with mobility change and presented the topological representation of variable mobility joints in the form of graphs and topology matrices. Xu et al. (2017) designed a metamorphic mechanism cell which can realize deploying, self-locking, unlocking, retracting and interlocking with

✉ Guoguang Jin
jinguoguang@tiangong.edu.cn

[1] School of Mechanical Engineering, Tiangong University, Tianjin 300387, China

[2] Tianjin Key Laboratory of Modern Electromechanical Equipment Technology, Tianjin 300387, China

other cells by incorporating variable kinematic joints. The study concluded that mechanisms can change their topology through the change of kinematic joints and special mechanism configurations.

However, the metamorphic mechanisms usually used for practical operation are the kind of constrained metamorphic mechanisms (Li et al. 2016). One of the metamorphosis operations is realized by using kinematic pair constraints, geometric constraints and/or force constraints to reduce the number of degrees of freedom (DOFs) of a multi-DOF metamorphic mechanism to the number of driving links. Then, the corresponding work configuration is built for the metamorphic mechanism. The approach to perform the intended working configuration using constrained metamorphic mechanisms is implemented by designing the constraint and structure types of metamorphic kinematic pair in order to provide the corresponding geometric constraints and/or force constraints. Zhang et al. (2010) presented metamorphic kinematic pair extracted from origami folds and investigated the topological reconfiguration and mobility change of the evolved parallel mechanism. Gan et al. (2009) created a new metamorphic joint called reconfigurable Hooke (rT) joint that changes the installation angle of the joint to form various structures of parallel mechanisms (Gan et al. 2010). Li et al. (2015) induced the concept of equivalent resistance of the constrained metamorphic mechanisms and investigated the constrained ways, characteristics and relationships of metamorphic joints.

The dynamics modeling of constrained metamorphic mechanisms is the basis of dynamic performance analysis, optimization design and control, and it is a problem that must be solved in practical application of constrained metamorphic mechanisms. To-this-date, great progress has been made in the study of kinematics and dynamics of metamorphic mechanisms. Jin et al. (2003, 2004) described different configurations of metamorphic mechanisms through the method of Huston lower-body arrays and gave the kinematics analyses with generalized topological structures including the velocity, angular velocity acceleration and angular acceleration. Valsamos et al. (2015) introduced a global kinematic measure for the evaluation of the emerging anatomies, of a given structure of a class of 3 DOF modular metamorphic manipulators. Gan et al. (2013, 2016a, b) presented unified forward and inverse kinematics modeling of metamorphic parallel mechanisms by combining geometric constraints. Zhang et al. (2016) conducted forward and inverse kinematics analysis of the parallel metamorphic mechanism in different configurations based on the unified mathematical model. Wang et al. (2017) established the nonlinear dynamics model of the novel control metamorphic palletizing robot mechanism considering the effect of damping. Though the configuration complete dynamics model of metamorphic mechanisms has been preliminarily established, it is only applicable to metamorphic mechanisms with geometric constraints and has certain limitations on metamorphic mechanisms with force constraints. Generally, constrained metamorphic operations of the constrained metamorphic mechanisms are implemented by using geometric constraints and/or force constraints of metamorphic joints to overlap two links to one or to make the metamorphic joints locked. Therefore, it is necessary to establish the unified dynamics model of constrained metamorphic mechanisms considering typical constraints (geometric constraints and/or force constraints).

Following the dynamics model, a numerical iterative algorithm is presented based on the theory that velocity and acceleration are same in an extremely brief period. As well known, the constrained metamorphic mechanisms are the kind of under-actuated mechanisms. Dynamics model of under-actuated mechanism is a kind of highly complex system of nonlinear differential–algebraic equations. For the problem of solving the equations, Katake et al. (2000) modified the Acrobot so as to impose holonomic constraints on the system. The problem of formulating the equations of motions of the system along with the holonomic constraints using traditional methods is then addressed. Xiong et al. (2015) reduced the under-actuated mechanisms to three subsystems with holonomic constraints by controlling the angles of the actuated links in stages and solved the target angles of actuated links by particle swarm optimization algorithm. The characteristic of this method is that different geometric constraints should be set for different mechanisms without considering force constraints. Considering constrained metamorphic mechanisms in this paper, the theory that velocity and acceleration are same in an extremely brief period shows a good way to solve the dynamic equations including both geometric constraints and force constraints.

This paper is arranged in the following structure. Section 2 presents a unified dynamics model of constrained metamorphic mechanisms according to the constitution theory of mechanisms. To solve the dynamic equations of constrained metamorphic mechanisms, a numerical iterative algorithm is proposed based on the theory that velocity and acceleration are same in an extremely brief period in Sect. 3. In Sect. 4, the planar double-folded metamorphic mechanism and the metamorphic nipper swing mechanism are introduced, and the computer numerical analysis and dynamic simulation are carried to demonstrate the proposed method. Finally, conclusions are drawn in Sect. 5.

2 Dynamics Model of Constrained Metamorphic Mechanisms

According to structural theory and formation methodology of metamorphic mechanisms based on augmented Assur groups (Li and Dai 2010), the constrained metamorphic mechanisms can be divided into four parts including

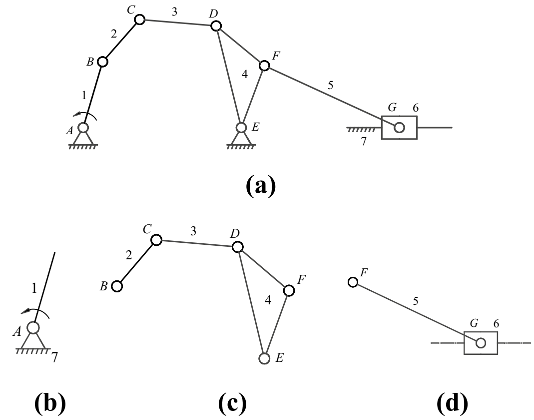

Fig. 1 The 2-DOF metamorphic mechanism and its composition principle

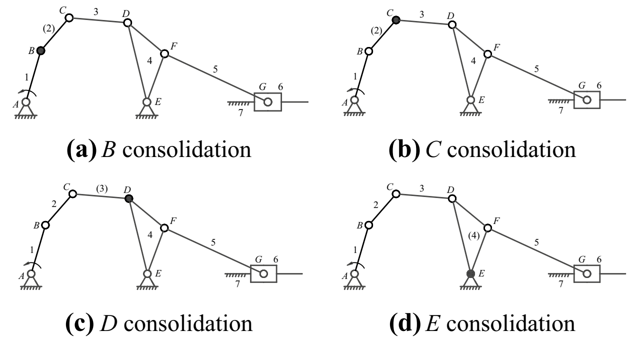

Fig. 2 Four metamorphic configurations of the 2-DOF metamorphic mechanism

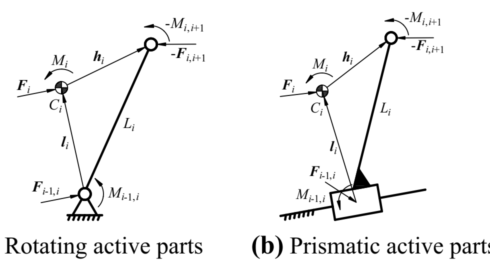

Fig. 3 Dynamic analysis of active parts

frame, active parts, several basic Assur groups and at least one augmented Assur groups. To illustrate the Assur group based metamorphic mechanisms, the 2-DOF metamorphic mechanism is taken as an example. The 2-DOF metamorphic mechanism is composed of active part, augmented Assur group RRRR and Assur group RRP (Fig. 1b, d) and its composition principle are shown in Fig. 1. The mechanism has two loops. The active part and frame are connected with augmented Assur group RRRR to form a loop. The other loop is composed of Assur group RRP connected to the former loop and frame.

The metamorphic process of mechanism based on augmented Assur group is the process of transforming 1-DOF augmented Assur group into basic Assur group. The 2-DOF metamorphic mechanism shown in Fig. 1 consists of an augmented Assur group, and its four metamorphic configurations are shown in Fig. 2.

According to the above-mentioned structural theory and formation methodology of metamorphic mechanisms based on augmented Assur groups, the unified dynamics modeling method of constrained metamorphic mechanism is studied.

2.1 Dynamics Model of Active Parts

The driving forms of active parts are shown in Fig. 3. Figure 3a and b shows active parts in pure rotational and pure prismatic form, respectively.

According to the Newton–Euler equation (referred to as N/E equation), the dynamic equations of active parts can be written as follows,

$$\begin{cases} \boldsymbol{F}_{i-1,i} - \boldsymbol{F}_{i,i+1} + \boldsymbol{F}_i = m_i \ddot{\boldsymbol{C}}_i \\ M_{i-1,i} - \boldsymbol{l}_i \times \boldsymbol{F}_{i-1,i} - M_{i,i+1} - \boldsymbol{h}_i \times \boldsymbol{F}_{i,i+1} + M_i = I_{C,i} \boldsymbol{\varepsilon}_i \end{cases} \quad (1)$$

where $\boldsymbol{F}_{i-1,i}$ and $\boldsymbol{F}_{i+1,i}$ are the force vectors at component L_i exerted by components L_{i-1} and L_{i+1}, respectively, and $\boldsymbol{F}_{i+1,i} = -\boldsymbol{F}_{i,i+1}$; $M_{i-1,i}$ and $M_{i+1,i}$ are the moments at component L_i exerted by components L_{i-1} and L_{i+1}, respectively, and $M_{i+1,i} = -M_{i,i+1}$; $\boldsymbol{F}_i$ is the external force vector acting on the component L_i; M_i is the external moment acting on the component L_i; $I_{C,i}$ is the moment of inertia of the component L_i around the centroid C_i; $\boldsymbol{\varepsilon}_i$ is the angular acceleration of the component L_i; $\ddot{\boldsymbol{C}}_i$ is the acceleration vector at the centroid of the component L_i.

2.2 Dynamics Model of the Assur Groups

The simplest Assur groups are a kind of Class II Assur groups composed of two components and three low pairs, and it is also the most widely used Assur group. In addition to Class II Assur groups, there are also higher-level Assur groups such as Class III and IV Assur groups. The dynamic analysis diagrams of Class II and III Assur group are given in Table 4 in "Appendix 1." According to the dynamic analysis of Assur group in Table 4 in "Appendix 1," the dynamic equation of the Class II Assur groups can be written based on N/E equation as follows,

$$\begin{cases} \boldsymbol{F}_{i-1,i} + \boldsymbol{F}_i - \boldsymbol{F}_{i+1,i+2} + \boldsymbol{F}_{i+1} = m_i \ddot{\boldsymbol{C}}_i + m_{i+1} \ddot{\boldsymbol{C}}_{i+1} \\ M_{i-1,i} - (\boldsymbol{l}_i + \boldsymbol{h}_i) \times \boldsymbol{F}_{i-1,i} + M_i - \boldsymbol{h}_i \times \boldsymbol{F}_i - M_{i,i+1} = I_{k-1,k} \boldsymbol{\varepsilon}_i \\ -M_{i+1,i+2} + (\boldsymbol{l}_{i+1} + \boldsymbol{h}_{i+1}) \times \boldsymbol{F}_{i+1,i+2} + M_{i+1} - \boldsymbol{h}_{i+1} \times \boldsymbol{F}_{i+1} \\ \quad + M_{i,i+1} = I_{k+1,k} \boldsymbol{\varepsilon}_{i+1} \end{cases} \quad (2)$$

where $I_{k-1,k}$ and $I_{k+1,k}$ are the moments of inertia of components L_i and L_{i+1} around the internal kinematic joint P_k, respectively.

Similarly, the dynamic equation of Class III Assur groups can be written as follows,

$$\begin{cases} \boldsymbol{F}_{n-1,i-1} + \boldsymbol{F}_{i-1} + \boldsymbol{F}_{n,i} + \boldsymbol{F}_{i} + \boldsymbol{F}_{n+1,i+1} + \boldsymbol{F}_{i+1} + \boldsymbol{F}_{i+2} = \sum_{n=-1}^{2} m_{i+n}\ddot{\boldsymbol{C}}_{i+n} \\ M_{n-1,i-1} - (\mathbf{l}_{i-1} + \mathbf{h}_{i-1}) \times \boldsymbol{F}_{n-1,i-1} + M_{i-1} - \mathbf{h}_{i-1} \times \mathbf{F}_{i-1} \\ \quad - M_{i-1,i+2} = I_{k-1}\boldsymbol{\varepsilon}_{i-1} \\ M_{n,i} - (\mathbf{l}_i + \mathbf{h}_i) \times \mathbf{F}_{n,i} + M_i - \mathbf{h}_i \times \mathbf{F}_i - M_{i,i+2} = I_k\boldsymbol{\varepsilon}_i \\ M_{n+1,i+1} - (\mathbf{l}_{i+1} + \mathbf{h}_{i+1}) \times \mathbf{F}_{n+1,i+1} + M_{i+1} - \mathbf{h}_{i+1} \times \mathbf{F}_{i+1} \\ \quad - M_{i+1,i+2} = I_{k+1}\boldsymbol{\varepsilon}_{i+1} \\ M_{i-1,i+2} - \mathbf{s}_{i-1} \times \mathbf{F}_{i-1,i+2} + M_{i,i+2} - \mathbf{s}_i \times \mathbf{F}_{i,i+2} + M_{i+1,i+2} \\ \quad - \mathbf{s}_{i+1} \times \mathbf{F}_{i+1,i+2} + M_{i+2} = I_{C,i+2}\ddot{\mathbf{C}}_{i+2} \end{cases} \tag{3}$$

where $\boldsymbol{F}_{n-1,i-1}$, $\boldsymbol{F}_{n,i}$ and $\boldsymbol{F}_{n+1,i+1}$ are the constraint force vectors at the external kinematic joints P_{k-1}, P_k and P_{k+1} exerted by components L_{i-1}, L_i and L_{i+1}, respectively; $M_{n-1,i-1}$, $M_{n,i}$ and $M_{n+1,i+1}$ are the constraint torques at the external kinematic joints P_{k-1}, P_k and P_{k+1} exerted by components L_{i-1}, L_i and L_{i+1}, respectively; I_{k-1}, I_k and I_{k+1} are the moments of inertia of components L_{i-1}, L_i and L_{i+1} around the internal kinematic joints Q_{k-1}, Q_k and Q_{k+1}, respectively; $I_{C,i+2}$ is the moment of inertia of the component L_{i+2} around the centroid C_{i+2}; $\boldsymbol{s}_{i-1}$, $\boldsymbol{s}_i$ and $\boldsymbol{s}_{i+1}$ are the radius vectors of the centroid C_{i+2} on the component L_{i+2} relative to the internal kinematic joints Q_{k-1}, Q_k and Q_{k+1}, respectively.

2.3 Dynamics Model of the Augmented Assur Groups

Since the constrained metamorphic mechanisms only implement metamorphism for the augmented Assur groups, the metamorphic process is realized by constraining the movement cycle of the metamorphic joints. Therefore, the kinematic characteristics of metamorphic joints should be considered in the dynamic analysis of the augmented Assur groups.

2.3.1 Analysis of Kinematic Characteristics of Metamorphic Joints

In order to effectively reflect the variation of constraint types of metamorphic joints during the metamorphic process, the equivalent resistance (Li et al. 2016) is introduced. Based on the functional requirements of the constrained metamorphic mechanisms at the different working configurations, the typical constraint forms and the corresponding kinematic characteristics of the metamorphic joints are analyzed, as shown in Table 1.

Wherein, j_1 denotes that the metamorphic joint is in the extreme position under the constraint form; j_2 denotes that the metamorphic joint is in the non-extreme position under the constraint form; c_1 represents a constant larger than or equal to 1, c_2 represents a constant less than or equal to 1, and the exact value can be obtained by reference (Li et al. 2016). As can be seen from Table 1, there are two kinds of kinematic characteristics of the metamorphic joints under different constraints corresponding to different equivalent resistances. When the constraint form of the metamorphic joint is geometric constraint and it is in the non-extreme position, the equivalent resistance is $f = 0$, and the metamorphic joint is in a relative moving state; when the constraint form of the metamorphic joint is geometric constraint and it is in the extreme position, the equivalent resistance is $f = \infty$, and the metamorphic joint is in a relative static state; when the constraint form of the metamorphic joint is force constraint and it is in the non-extreme position, the equivalent resistance is $f = c_2$, and the metamorphic joint is in a relative moving state; when the constraint form of the metamorphic joint is force constraint and it is in the extreme position, the equivalent resistance is $f = c_1$, and the metamorphic joint is in a relative static state.

2.3.2 Configuration Division of the Augmented Assur Groups

Assuming that any kinematic joints in the augmented Assur groups may be metamorphic joints, it can be seen from Table 1 that the metamorphic joints exist relative moving and relative static states under different equivalent

Table 1 Analysis of kinematic characteristics of metamorphic joints under typical constraints

Constraint forms	Mechanism configuration	The equivalent resistance	Kinematic characteristics
Geometric constraint	j_1	$f = \infty$	Relative static
	j_2	$f = 0$	Relative moving
Force constraint	j_1	$f = c_1$	Relative static
	j_2	$f = c_2$	Relative moving
Combination constraint	j_1	$f = \infty$	Relative static
	j_2	$f = c_2$	Relative moving

resistances. Therefore, the configuration of the augmented Assur groups can be divided as follows,

(1) When the two components connected by the metamorphic joints in the augmented Assur groups move relative to each other, the augmented Assur groups can be divided into one Assur groups and one component with two pairs. The mechanism is in the non-extreme position, and such a configuration is named non-collision configuration.
(2) When the two components connected by the metamorphic joints in the augmented Assur groups are relatively static, the augmented Assur groups are degenerated into the corresponding equivalent Assur groups. The mechanism is in the extreme position; if the metamorphosis occurs in the internal kinematic joints, it is the internal collision configuration; if the metamorphosis occurs in the external kinematic joints, it is the external collision configuration.

2.3.3 Dynamic Analysis of the Augmented Assur Groups

The augmented Assur group RRRR is taken as an example. When the augmented Assur group RRRR is in the non-collision configuration, it is shown in Fig. 4. Combining with the analysis of kinematic characteristics in Table 1 and the force analysis in Table 5 in "Appendix 2," the dynamic equation of Class II augmented Assur groups in the non-collision configuration based on the N/E equation can be written as follows,

$$\begin{cases} \boldsymbol{F}_{k-1} + \mathbf{F}_{i-1,i} + \mathbf{F}_i - \mathbf{F}_{i+1,i+2} - \mathbf{F}_{k+1} + \mathbf{F}_{i+1} = m_i \ddot{\mathbf{C}}_i + m_{i+1}\ddot{\mathbf{C}}_{i+1} \\ M_{k-1} + M_{i-1,i} - (\mathbf{l}_i + \mathbf{h}_i) \times (\boldsymbol{F}_{k-1} + \mathbf{F}_{i-1,i}) + M_i \\ \quad - \mathbf{h}_i \times \mathbf{F}_i - M_{i,i+1} - M_k = I_{k-1,k}\boldsymbol{\varepsilon}_i \\ -M_{k+1} - M_{i+1,i+2} + (\mathbf{l}_{i+1} + \mathbf{h}_{i+1}) \times (\mathbf{F}_{k+1} + \mathbf{F}_{i+1,i+2}) + M_{i+1} \\ \quad - \mathbf{h}_{i+1} \times \mathbf{F}_{i+1} + M_{i,i+1} + M_k = I_{k+1,k}\boldsymbol{\varepsilon}_{i+1} \\ \mathbf{F}_{i+1,i+2} + \mathbf{F}_{k+1} + \mathbf{F}_{i+2} - \mathbf{F}_{i+2,i+3} - \mathbf{F}_{k+2} = m_{i+2}\ddot{\mathbf{C}}_{i+2} \\ -M_{k+2} - M_{i+2,i+3} + \left(\mathbf{l}_{i+2} + \mathbf{h}_{i+2}\right) \times (\mathbf{F}_{k+2} + \mathbf{F}_{i+2,i+3}) + M_{i+2} \\ \quad - \mathbf{h}_{i+2} \times \mathbf{F}_{i+2} + M_{i+1,i+2} + M_{k+1} = I_{k+2,k+1}\boldsymbol{\varepsilon}_{i+2} \end{cases} \tag{4}$$

where $\boldsymbol{F}_{k-1}$, $\boldsymbol{F}_k$, $\boldsymbol{F}_k$ and $\boldsymbol{F}_{k+2}$ are the internal constraint forces added to the kinematic joints P_{k-1}, P_k, P_{k+1} and P_{k+2}, respectively; M_{k-1}, M_k, M_{k+1} and M_{k+2} are the internal constraint torques added to kinematic joints P_{k-1}, P_k, P_{k+1} and P_{k+2}, respectively.

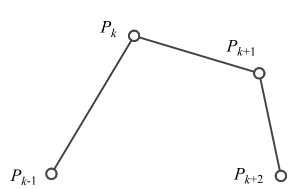

Fig. 4 Non-collision configuration

When the augmented Assur group RRRR is in the internal collision configuration (as shown in Fig. 5), there is no relative moving between the two members connected by the metamorphic joints, and then the dynamic equation of Class II augmented Assur groups is,

$$\begin{cases} \mathbf{F}_{i-1,i} + \sum_{n=0}^{2} \mathbf{F}_{i+n} - \mathbf{F}_{i+2,i+3} - \boldsymbol{F}_{k-1} - \mathbf{F}_{k+2} = \sum_{n=0}^{2} m_{i+n}\ddot{\mathbf{C}}_{i+n} \\ M_{k-1} + M_{i-1,i} - (\mathbf{l}_i + \mathbf{h}_i) \times (\boldsymbol{F}_{k-1} + \mathbf{F}_{i-1,i}) + M_i \\ \quad - \mathbf{h}_i \times \mathbf{F}_i - M_{i,i+1} - M_k = I_{k-1,k}\boldsymbol{\varepsilon}_i \\ (\mathbf{l}_{i+2} + \mathbf{h}_{i+2} + \mathbf{l}_{i+1} + \mathbf{h}_{i+1}) \times (\mathbf{F}_{i+2,i+3} + \mathbf{F}_{k+2}) - M_{k-2} - M_{i+2,i+3} \\ \quad - (\mathbf{h}_{i+2} + \mathbf{l}_{i+1} + \mathbf{h}_{i+1}) \times \mathbf{F}_{i+2} + M_{i+2} + M_{i+1} - \mathbf{h}_{i+1} \times \mathbf{F}_{i+1} \\ \quad + M_{i,i+1} + M_k = I_{k+1,k}\boldsymbol{\varepsilon}_{i+1} + I_{k+2,k+1}\boldsymbol{\varepsilon}_{i+2}. \end{cases} \tag{5}$$

Similarly, the dynamic equation of Class II augmented Assur groups in the external collision configuration (as shown in Fig. 6) can be expressed as,

$$\begin{cases} \boldsymbol{F}_{k-1} + \mathbf{F}_{i-1,i} + \mathbf{F}_i - \mathbf{F}_{i+1,i+2} - \mathbf{F}_{k+1} + \mathbf{F}_{i+1} = m_i \ddot{\mathbf{C}}_i + m_{i+1}\ddot{\mathbf{C}}_{i+1} \\ M_{k-1} + M_{i-1,i} - (\mathbf{l}_i + \mathbf{h}_i) \times (\boldsymbol{F}_{k-1} + \mathbf{F}_{i-1,i}) + M_i \\ \quad - \mathbf{h}_i \times \mathbf{F}_i - M_{i,i+1} - M_k = I_{k-1,k}\boldsymbol{\varepsilon}_i \\ -M_{k+1} - M_{i+1,i+2} + (\mathbf{l}_{i+1} + \mathbf{h}_{i+1}) \times (\mathbf{F}_{k+1} + \mathbf{F}_{i+1,i+2}) + M_{i+1} \\ \quad - \mathbf{h}_{i+1} \times \mathbf{F}_{i+1} + M_{i,i+1} + M_k = I_{k+1,k}\boldsymbol{\varepsilon}_{i+1} \end{cases} \tag{6}$$

The augmented Assur group RR-RR-RR-R is taken as an example. When the augmented Assur group RR-RR-RR-R is in the non-collision configuration, it is shown in Fig. 7. Combining with the analysis of kinematic characteristics in Table 1 and the force analysis Table 5 in "Appendix 2," the

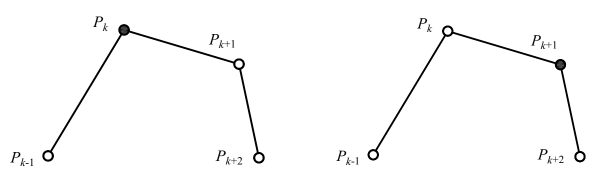

(a) P_k consolidation **(b)** P_{k+1} consolidation

Fig. 5 Internal collision configuration

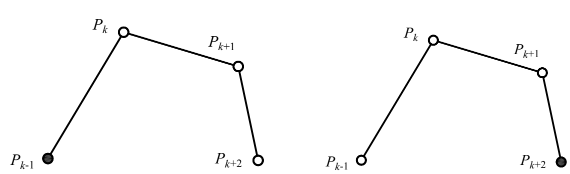

(a) P_{k-1} consolidation **(b)** P_{k+2} consolidation

Fig. 6 External collision configuration dynamic equation of Class III augmented Assur groups in the non-collision configuration can be written as,

$$
\begin{cases}
\boldsymbol{F}_{n-1,i-1} - \boldsymbol{F}_{i,i+3} + \boldsymbol{F}_{n+1,i+1} + \sum\limits_{n=-1}^{2} \boldsymbol{F}_{i+n} + \boldsymbol{F}_{k-1} - \boldsymbol{F}_{k} \\
\quad + \boldsymbol{F}_{k+1} = \sum\limits_{n=-1}^{2} m_{i+n}\ddot{\boldsymbol{C}}_{i+n} \\
M_{n-1,i-1} + M_{k-1} - (\mathbf{l}_{i-1} + \mathbf{h}_{i-1}) \times (\boldsymbol{F}_{n-1,i-1} + \mathbf{F}_{k-1}) + M_{i-1} \\
\quad - \mathbf{h}_{i-1} \times \mathbf{F}_{i-1} - M_{i-1,i+2} - M_{q,k-1} = I_{k-1}\boldsymbol{\varepsilon}_{i-1} \\
-M_{k} - M_{i,i+3} + (\mathbf{l}_{i} + \mathbf{h}_{i}) \times (\mathbf{F}_{k} + \mathbf{F}_{i,i+3}) + M_{i} \\
\quad - \mathbf{h}_{i} \times \mathbf{F}_{i} - M_{i,i+2} - M_{q,k} = I_{k}\boldsymbol{\varepsilon}_{i} \\
M_{n+1,i+1} + M_{k+1} - (\mathbf{l}_{i+1} + \mathbf{h}_{i+1}) \times \left(\mathbf{F}_{n+1,i+1} + \mathbf{F}_{k+1}\right) \\
\quad + M_{i+1} - \mathbf{h}_{i+1} \times \mathbf{F}_{i+1} - M_{i+1,i+2} - M_{q,k+1} = I_{k+1}\boldsymbol{\varepsilon}_{i+1} \\
M_{q,k-1} + M_{i-1,i+2} - \mathbf{s}_{i-1} \times \mathbf{F}_{i-1,i+2} + M_{q,k} + M_{i,i+2} - \mathbf{s}_{i} \times \mathbf{F}_{i,i+2} \\
\quad + M_{q,k+1} + M_{i+1,i+2} - \mathbf{s}_{i+1} \times \mathbf{F}_{i+1,i+2} + M_{i+2} = I_{C,i+2}\boldsymbol{\varepsilon}_{i+2} \\
\mathbf{F}_{i,i+3} + \mathbf{F}_{i+3} + \mathbf{F}_{n+3,i+3} + \mathbf{F}_{k} - \mathbf{F}_{k+2} = m_{i+3}\ddot{\boldsymbol{C}}_{i+3} \\
M_{n+3,i+3} - M_{k+2} - \left(\mathbf{l}_{i+3} + \mathbf{h}_{i+3}\right) \times \left(\mathbf{F}_{n+3,i+3} - \mathbf{F}_{k+2}\right) \\
\quad + M_{i+3} - \mathbf{h}_{i+3} \times \mathbf{F}_{i+3} + M_{k} + M_{i,i+3} = I_{k+2,k}\boldsymbol{\varepsilon}_{i+3}
\end{cases}
\tag{7}
$$

where $M_{q,k-1}$, $M_{q,k}$ and $M_{q,k+1}$ are the internal constraint torques added to kinematic joints Q_{k-1}, Q_k and Q_{k+1}, respectively.

The dynamic equation of Class III augmented Assur groups in the internal collision configuration (as shown in Fig. 8) can be expressed as,

$$
\begin{cases}
\boldsymbol{F}_{n-1,i-1} + \boldsymbol{F}_{k-1} + \boldsymbol{F}_{n+1,i+1} + \boldsymbol{F}_{k+1} + \boldsymbol{F}_{n+3,i+3} - \boldsymbol{F}_{k+2} \\
\quad + \sum\limits_{n=-1}^{3} \boldsymbol{F}_{i+n} = \sum\limits_{n=-1}^{3} m_{i+n}\ddot{\boldsymbol{C}}_{i+n} \\
M_{n-1,i-1} + M_{k-1} - (\mathbf{l}_{i-1} + \mathbf{h}_{i-1}) \times (\boldsymbol{F}_{n-1,i-1} + \mathbf{F}_{k-1}) + M_{i-1} \\
\quad - \mathbf{h}_{i-1} \times \mathbf{F}_{i-1} - M_{i-1,i+2} - M_{q,k-1} = I_{k-1}\boldsymbol{\varepsilon}_{i-1} \\
M_{n+3,i+3} - M_{k+2} - (\mathbf{l}_{i+3} + \mathbf{h}_{i+3} + \mathbf{l}_{i} + \mathbf{h}_{i}) \times (\mathbf{F}_{n+3,i+3} - \mathbf{F}_{k+2}) \\
\quad + M_{i+3} - (\mathbf{h}_{i+3} + \mathbf{l}_{i} + \mathbf{h}_{i}) \times \mathbf{F}_{i+3} + M_{i} + \mathbf{h}_{i} \times \mathbf{F}_{i} \\
\quad - M_{i,i+2} - M_{q,k} = I_{k+2,k}\boldsymbol{\varepsilon}_{i+3} + I_{k}\boldsymbol{\varepsilon}_{i} \\
M_{n+1,i+1} + M_{k+1} - (\mathbf{l}_{i+1} + \mathbf{h}_{i+1}) \times \left(\mathbf{F}_{n+1,i+1} + \mathbf{F}_{k+1}\right) + M_{i+1} \\
\quad - \mathbf{h}_{i+1} \times \mathbf{F}_{i+1} - M_{i+1,i+2} - M_{q,k+1} = I_{k+1}\boldsymbol{\varepsilon}_{i+1} \\
M_{i-1,i+2} - \mathbf{s}_{i-1} \times \mathbf{F}_{i-1,i+2} + M_{i,i+2} - \mathbf{s}_{i} \times \mathbf{F}_{i,i+2} + M_{i+1,i+2} \\
\quad - \mathbf{s}_{i+1} \times \mathbf{F}_{i+1,i+2} + M_{i+2} + M_{q,k-1} + M_{q,k} + M_{q,k+1} = I_{i+2}\boldsymbol{\varepsilon}_{i+2}.
\end{cases}
\tag{8}
$$

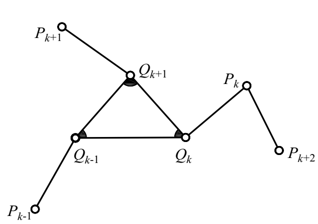

Fig. 7 Non-collision configuration

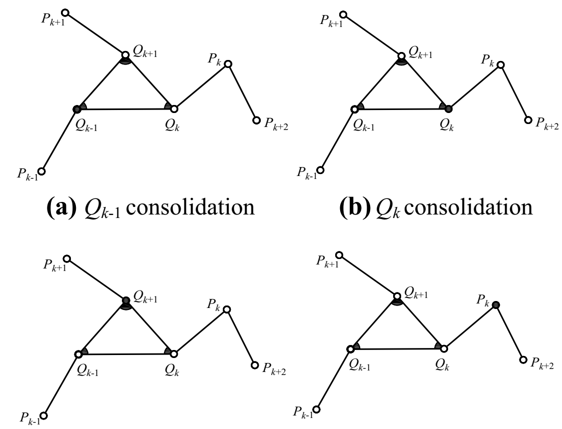

(a) Q_{k-1} consolidation **(b)** Q_k consolidation

(c) Q_{k+1} consolidation **(d)** P_k consolidation

Fig. 8 Internal collision configuration

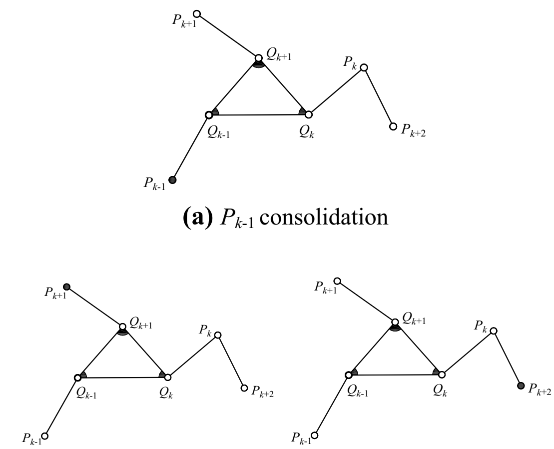

(a) P_{k-1} consolidation

(b) P_{k+1} consolidation **(c)** P_{k+2} consolidation

Fig. 9 External collision configuration

The dynamic equation of Class III augmented Assur groups in the external collision configuration (as shown in Fig. 9) can be expressed as,

$$
\begin{cases}
\boldsymbol{F}_{n-1,i-1} - \boldsymbol{F}_{i,i+3} + \boldsymbol{F}_{n+1,i+1} + \sum\limits_{n=-1}^{2} \boldsymbol{F}_{i+n} + \boldsymbol{F}_{k-1} - \boldsymbol{F}_{k} \\
\quad + \boldsymbol{F}_{k+1} = \sum\limits_{n=-1}^{2} m_{i+n}\ddot{\boldsymbol{C}}_{i+n} \\
M_{n-1,i-1} + M_{k-1} - (\mathbf{l}_{i-1} + \mathbf{h}_{i-1}) \times (\boldsymbol{F}_{n-1,i-1} + \mathbf{F}_{k-1}) + M_{i-1} \\
\quad - \mathbf{h}_{i-1} \times \mathbf{F}_{i-1} - M_{i-1,i+2} - M_{q,k-1} = I_{k-1}\boldsymbol{\varepsilon}_{i-1} \\
-M_{k} - M_{i,i+3} + (\mathbf{l}_{i} + \mathbf{h}_{i}) \times (\mathbf{F}_{k} + \mathbf{F}_{i,i+3}) + M_{i} - \mathbf{h}_{i} \times \mathbf{F}_{i} \\
\quad - M_{i,i+2} - M_{q,k} = I_{k}\boldsymbol{\varepsilon}_{i} \\
M_{n+1,i+1} + M_{k+1} - (\mathbf{l}_{i+1} + \mathbf{h}_{i+1}) \times \left(\mathbf{F}_{n+1,i+1} + \mathbf{F}_{k+1}\right) + M_{i+1} \\
\quad - \mathbf{h}_{i+1} \times \mathbf{F}_{i+1} - M_{i+1,i+2} - M_{q,k+1} = I_{k+1}\boldsymbol{\varepsilon}_{i+1} \\
M_{i-1,i+2} - \mathbf{s}_{i-1} \times \mathbf{F}_{i-1,i+2} + M_{i,i+2} - \mathbf{s}_{i} \times \mathbf{F}_{i,i+2} - \mathbf{s}_{i+1} \times \mathbf{F}_{i+1,i+2} \\
\quad + M_{i+1,i+2} + M_{i+2} + M_{q,k-1} + M_{q,k} + M_{q,k+1} = I_{C,i+2}\boldsymbol{\varepsilon}_{i+2}.
\end{cases}
\tag{9}
$$

The augmented Assur groups and/or Assur groups together constitute the groups of the constrained metamorphic mechanisms, and the connection relations and rules of the mechanism are the same as those of the traditional Assur groups. Therefore, the obtained dynamics models of the active parts, the Assur groups and the augmented Assur groups are generalized to the modular mathematical framework, and the unified dynamics model of constrained metamorphic mechanisms is established, which can be expressed in matrix form as,

$$\boldsymbol{M}\ddot{\boldsymbol{q}} + \boldsymbol{C} = \boldsymbol{h} + \boldsymbol{f} \tag{10}$$

where $\boldsymbol{M}$ is symmetric positive definite inertia matrix, $\ddot{\boldsymbol{q}}$ is generalized acceleration terms, $\boldsymbol{C}$ is the Coriolis force and centrifugal force terms, $\boldsymbol{h}$ is the generalized force terms, and $\boldsymbol{f}$ is the constraint force terms.

3 Specific Solution Process for Dynamics of Constrained Metamorphic Mechanisms

Assuming that the DOF of constrained metamorphic mechanisms is N_1, the number of active parts N_2, and the number of dynamic equations N_3, the dynamic equation of constrained metamorphic mechanisms shown in Eq. (10) is a mixed differential–algebraic equation, which contains (N_1–N_2) differential variables and $(N_3 - N_1 + N_2)$ algebraic variables. In the course of solution, the expression of algebraic variable about differential variable can be obtained by choosing arbitrarily $(N_3 - N_1 + N_2)$ equations in the dynamic equations. Subsequently, the expression of algebraic variable about differential variable is replaced by the remaining (N_1–N_2) dynamic equations, which are transformed into highly complex nonlinear differential equations. To solve this problem, a numerical iterative method for solving such differential linear equations is proposed. When the motion law of active parts and the initial position of the differential variables are given, the motion law of each component, the driving force/torque of active parts and the constraint force/torque of metamorphic joints can be obtained through iteration. The iteration process is described as follows.

3.1 Kinematics and Dynamics at Time t_0

There is a hypothesis at the initial moment t_0.

(1) The input positions of active parts are known, recorded as $q_i(t_0)$, $i = 1, 2, 3, \cdots, N_2$; the initial positions of differential variables are known, recorded as $q_j(t_0)$, $j = N_2 + 1, \cdots, N_2 + N_1$. Using the kinematic position equations of constrained metamorphic mechanisms, $q_k(t_0)$ can be obtained, $k = N_1 + N_2 + 1, \cdots, N_1 + N_2 + N_3$.

(2) At the initial moment, the velocities of active parts are $\dot{q}_i(t_0)$, and the velocities of differential variables are $\dot{q}_j(t_0)$. Base on step (1), $\dot{q}_k(t_0)$ can be obtained by using the kinematic velocity equations.

(3) The input accelerations of active parts are known, recorded as $\ddot{q}_i(t_0)$; Based on steps (1) and (2), the nonlinear differential equation can be used to obtain the accelerations of differential variables, recorded as $\ddot{q}_j(t_0)$. Then, the obtained results are introduced into the expressions of algebraic variables about differential variables, and the driving force/torque of the active parts and the constraint force/torque of the metamorphic joints can be obtained.

(4) On the basis of steps (1) to (3), $\ddot{q}_i(t_0)$ and $\ddot{q}_j(t_0)$ are introduced into the kinematic acceleration equations, and $\ddot{q}_k(t_0)$ can be obtained.

3.2 Kinematics and Dynamics at Time T_n

Let the time interval from time t_{n-1} to time t_n be infinitely small, denoted as δt. It can be considered that velocity and acceleration of the differential variable are constant within an infinitesimal time interval, which is equal to velocity and acceleration of the previous moment in the interval, and the interval velocity and acceleration at different time are changed by steps. There are several situations at time $t_n (n = 1, 2, 3, \cdots)$.

(1) The input positions of active parts are known, recorded as $q_i(t_n)$; the initial positions of differential variables are known, recorded as $q_j(t_n)$ and $q_j(t_n) = q_j(t_{n-1}) + \dot{q}_j(t_{n-1})\delta t$. Using the kinematic position equations of constrained metamorphic mechanisms, $q_k(t_n)$ can be obtained.

(2) The velocities of active parts are known, recorded as $\dot{q}_i(t_n)$; the velocities of differential variables are known, recorded as $\dot{q}_j(t_n)$. $\dot{q}_j(t_n) = \dot{q}_j(t_{n-1}) + \ddot{q}_j(t_{n-1})\delta t$ can be obtained based on the results at time t_{n-1}. $\dot{q}_k(t_n)$ can be obtained by using the kinematic velocity equations.

(3) The input accelerations of active parts are known, recorded as $\ddot{q}_i(t_n)$; the accelerations of differential variables $\ddot{q}_j(t_n)$ can be obtained by nonlinear differential equations, and they are introduced into the expression of algebraic variables about differential variables. The driving force/torque of the active parts and the constraint force/torque of the metamorphic joints can be obtained.

(4) Substituting $\ddot{q}_i(t_n)$ and $\ddot{q}_j(t_n)$ into the kinematic acceleration equations, $\ddot{q}_k(t_n)$ can be obtained.

According to the above steps, the position, velocity, acceleration, the driving force/torque of active parts and the constrained force/torque of metamorphic joints can be obtained at time t_n by iteration.

The iteration flowchart is shown in Fig. 10.

4 Simulation Examples

4.1 The Planar Double-Folded Metamorphic Mechanism

Taking the planar double-folded metamorphic mechanism (Wang and Dai 2007) as an example, the types and constraints of metamorphic joints based on the kinematic characteristics of metamorphic joints are given. According to the working task, the planar double-folded metamorphic mechanism (as shown in Fig. 11) must complete three working requirements: horizontal folding, vertical folding and reset.

(1) Horizontal folding, as shown in Fig. 11a, horizontally pushing the left side of the single-layer cardboard and rotating the second side of the left side along the second crease to vertical position.
(2) Vertical folding, as shown in Fig. 11b, completing the rotation of the first surface around the first crease and coinciding with the second surface.
(3) Reset, as shown in Fig. 11c, the mechanism returns to its initial position.

Figure 12 shows the schematic diagram of the planar double-folded metamorphic mechanism and its composition principle. According to the above requirements, force metamorphism is adopted at kinematic joint D, that is, when the mechanism is in configuration 1, the spring force is set at kinematic joint D, so that the relative moving resistance between the components 3 and 4 is larger than the motion resistance of the slider, and it keeps the components 3 and 4 relatively static. When the mechanism is in configuration 2, a geometric constraint is added at kinematic joint E, so that the slider moves to the specified position and stops moving when the mechanism meets the geometric limit. When the mechanism is in configuration 3, the spring force at kinematic joint D makes the components 3 and 4 to be relatively static. Based on the principle of augmented Assur groups, the planar double-folded metamorphic mechanism is divided into a fixed-axis rotating active part and an augmented Assur group RRRP (Fig. 12b and c).

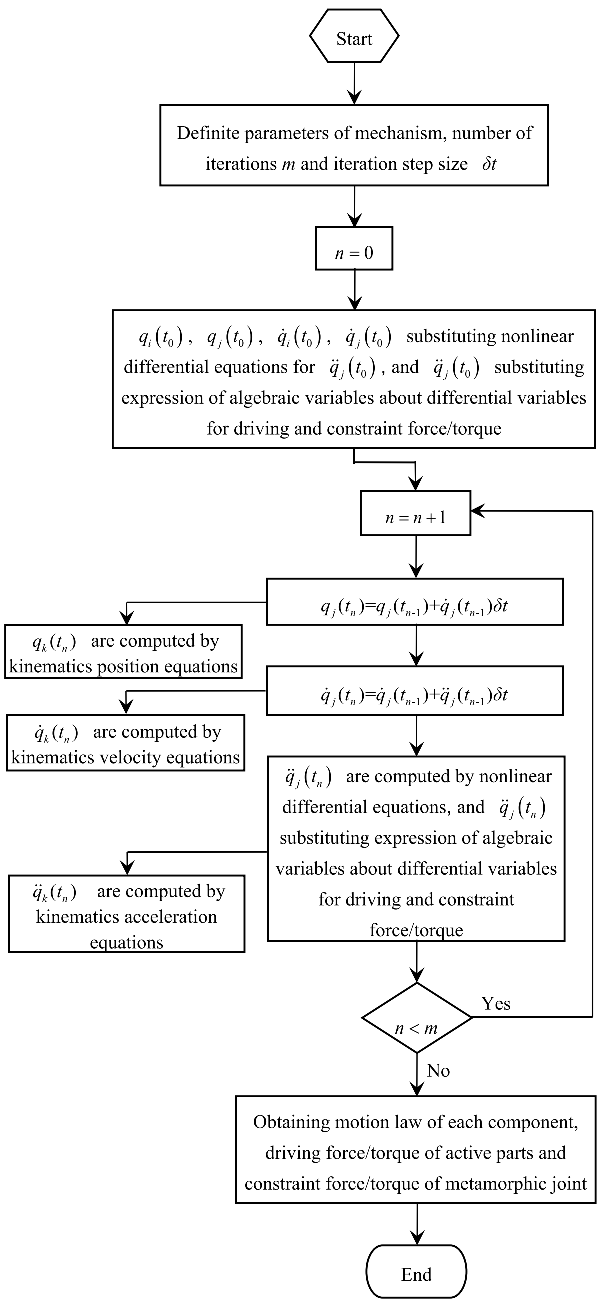

Fig. 10 The flowchart for numerical iterative algorithm

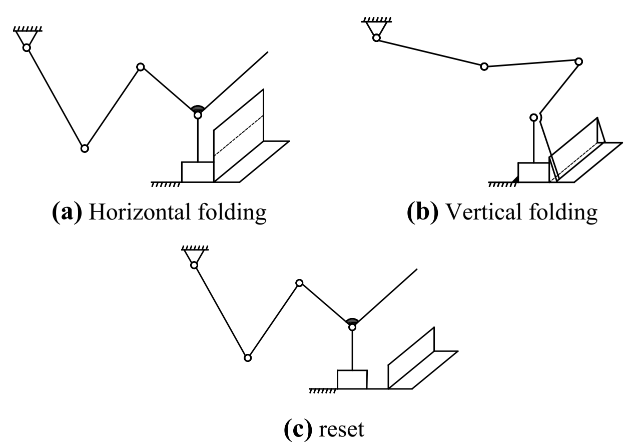

Fig. 11 The planar double-folded metamorphic mechanism

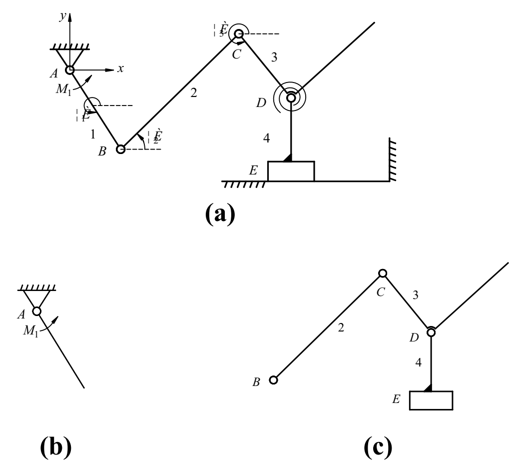

Fig. 12 The schematic diagram

Table 2 Geometric and inertia properties of the planar double-folded metamorphic mechanism (SI units)

Parameter	Measurement value	Parameter	Measurement value
L_{AB}	0.08	m_2	0.165
L_{BC}	0.2	m_3	0.162
L_{CD}	0.9	m_4	0.455
L_{AEy}	0.1425	J_1	1.8×10^{-4}
l_3	0.06	J_{BC}	2.3×10^{-3}
l_4	0.078	J_{DC}	8.8×10^{-4}
α_3	0.424	k	$3.24/\pi$
m_1	0.075	c	$0.18/\pi$

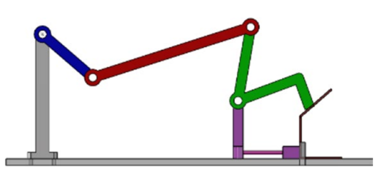

Fig. 13 Three-dimensional graph

According to the geometric and physical parameters of the planar double-folded metamorphic mechanism in Table 2, a three-dimensional model is established in SolidWorks, as shown in Fig. 13. The initial location of component 4 is 227.73 mm, and the initial position of the component 1 is π rad.

Assuming that the active part 1 rotates at a constant speed of 6 r/min (motion period is 10 s), the dynamic simulation is carried out in SolidWorks virtual prototype environment, and the relationship between the driving torque and time of the planar double-folded metamorphic mechanism is obtained.

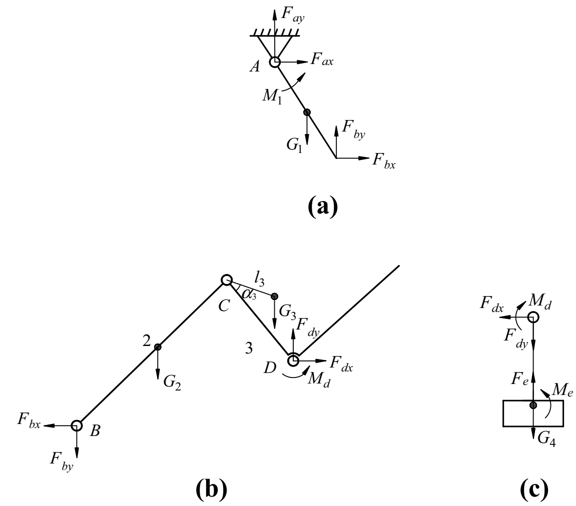

Fig. 14 Dynamic analysis in configurations 1 and 3

When the planar double-folded metamorphic mechanism is in configurations 1 and 3, the mechanism under force constraint can be regarded as consisting of an active part and an augmented Assur group RRRP (as shown in Fig. 12b and c). The dynamic analysis of the planar double-folded metamorphic mechanism in configurations 1 and 3 is shown in Fig. 14.

The dynamic equations in configurations 1 and 3 can be obtained by Eqs. (1) and (4) as follows,

$$\begin{cases} F_{ax}+F_{bx}=m_1a_{1x} \\ F_{ay}+F_{by}-G_1=m_1a_{1y} \\ 0.5L_{AB}F_{bx}\sin(\theta_1-\pi)+0.5L_{AB}F_{by}\cos(\theta_1-\pi)+M_1 \\ \quad -0.5L_{AB}F_{ax}\sin(\theta_1-\pi)-0.5L_{AB}F_{ay}\cos(\theta_1-\pi)=J_1\ddot{\theta}_1 \end{cases} \tag{11}$$

$$\begin{cases} -F_{bx}+F_{dx}=m_2a_{2x}+m_3a_{3x} \\ -F_{by}+F_{dy}-G_2-G_3=m_2a_{2y}+m_3a_{3y} \\ -L_{BC}F_{bx}\sin\theta_2+L_{BC}F_{by}\cos\theta_2+0.5L_{BC}G_2\cos\theta_2=J_{BC}\ddot{\theta}_2 \\ -L_{CD}F_{dx}\sin\theta_3+L_{CD}F_{dy}\cos\theta_3-G_3l_3\cos(\theta_3+\alpha_3)+M_d=J_{DC}\ddot{\theta}_3 \\ -F_{dx}=m_4a_{4x} \\ -F_{dy}+F_e-G_4=m_4a_{4y} \\ l_4F_{dx}+M_e-M_d=0. \end{cases} \tag{12}$$

When the mechanism is in configuration 2, the mechanism under geometric constraint can be regarded as consisting of an active part and an Assur group RRR, as shown in Fig. 15. The dynamic analysis of the planar double-folded metamorphic mechanism in configuration 2 is shown in Fig. 14a and b. The dynamic equations in configuration 2 can be obtained by Eqs. (1) and (6) as follows,

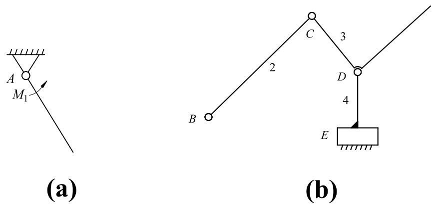

Fig. 15 Configuration 2

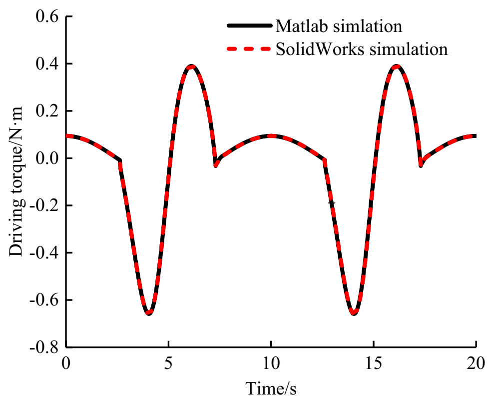

Fig. 16 Driving torque of the planar double-folded metamorphic mechanism

$$\begin{cases} F_{ax} + F_{bx} = m_1 a_{1x} \\ F_{ay} + F_{by} - G_1 = m_1 a_{1y} \\ 0.5L_{AB} F_{bx} \sin(\theta_1 - \pi) + 0.5L_{AB} F_{by} \cos(\theta_1 - \pi) + M_1 \\ \quad - 0.5L_{AB} F_{ax} \sin(\theta_1 - \pi) - 0.5L_{AB} F_{ay} \cos(\theta_1 - \pi) = J_1 \ddot{\theta}_1 \end{cases} \tag{13}$$

$$\begin{cases} -F_{bx} + F_{dx} = m_2 a_{2x} + m_3 a_{3x} \\ -F_{by} + F_{dy} - G_2 - G_3 = m_2 a_{2y} + m_3 a_{3y} \\ -L_{BC} F_{bx} \sin\theta_2 + L_{BC} F_{by} \cos\theta_2 + 0.5L_{BC} G_2 \cos\theta_2 = J_{BC} \ddot{\theta}_2 \\ -L_{CD} F_{dx} \sin\theta_3 + L_{CD} F_{dy} \cos\theta_3 - G_3 l_3 \cos(\theta_3 + \alpha_3) + M_d = J_{DC} \ddot{\theta}_3. \end{cases} \tag{14}$$

The parameters in Table 2 are substituted into the dynamic equations of the planar double-folded metamorphic mechanism, and the numerical iterative algorithm is adopted (the iteration time step is 0.01 s). The relationship between driving torque and time is obtained by using Matlab numerical simulation software. The results are compared with those of SolidWorks virtual dynamics simulation. As shown in Fig. 16, the numerical results of driving torque are in good agreement with those of virtual simulation. It verifies the correctness and validity of the dynamics model for Class II augmented Assur groups and solves the difficult problem of solving the dynamics model of constrained metamorphic mechanisms due to the existence of non-holonomic constraints and strong coupling.

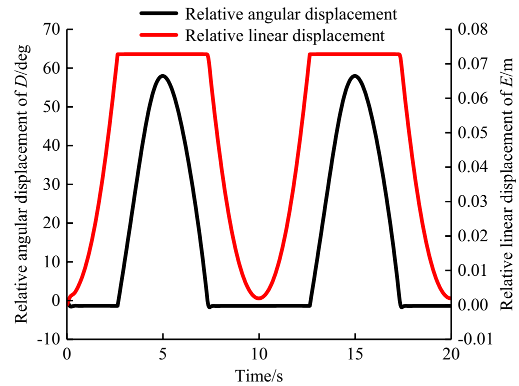

Fig. 17 The relative motion laws of metamorphic joints

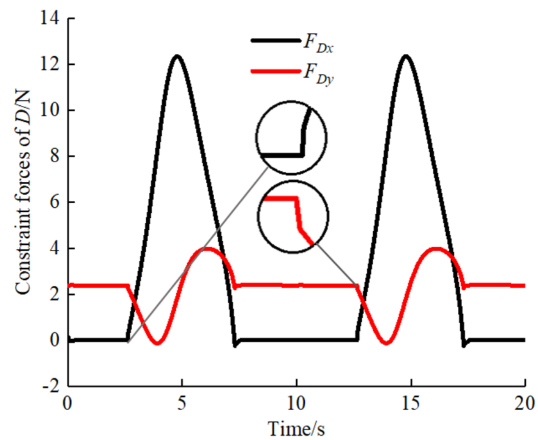

Fig. 18 The constraint forces of metamorphic joint D

In addition, the relative motion law and the constraint force/torque of the metamorphic joints of the planar double-folded metamorphic mechanism in two working cycles can be obtained by numerical calculation, as shown in Figs. 17, 18 and 19.

Figure 17 shows that the planar double-folded metamorphic mechanism is in horizontal folding state within 0–2.63 s, in which metamorphic joint D is relatively static and metamorphic joint E is relatively moving; the planar double-folded metamorphic mechanism is in vertical folding state within 2.63–7.3 s, in which metamorphic joint D is relatively moving and metamorphic joint E is relatively static; the planar double-folded metamorphic mechanism is in reset state within 7.3–10 s, in which metamorphic joint D is relatively static and metamorphic joint E is relatively moving. At the same time, it can be seen from Fig. 17 that the relative angular displacement of the metamorphic joint D and the relative linear displacement of the metamorphic joint E have a sudden change at the initial moment. The sudden change is related to the initial position of the torsional spring. The

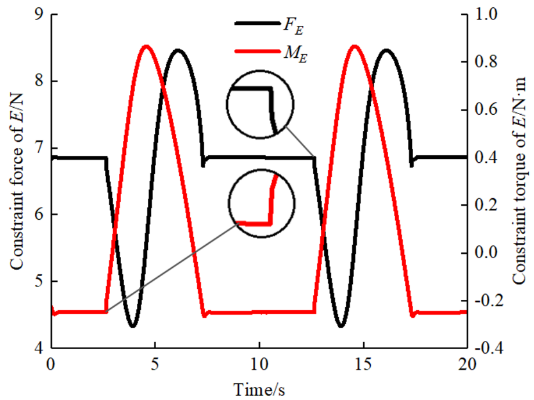

Fig. 19 The constraint force/torque of metamorphic joint E

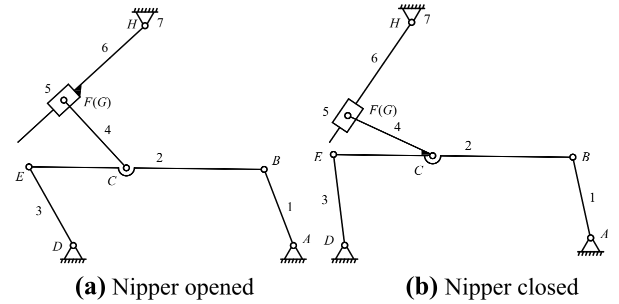

Fig. 20 Working configuration of the metamorphic nipper swing mechanism

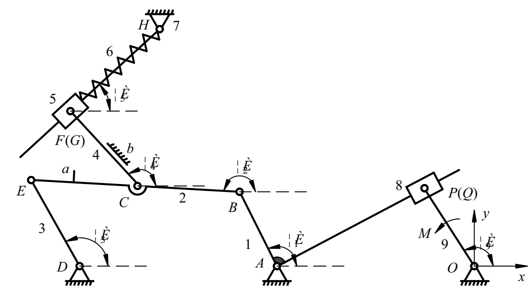

Fig. 21 The schematic diagram

deformation of the torsional spring can be obtained by static analysis of the mechanism at the initial moment of configuration 1; thus, the sudden change of metamorphic joint can be avoided at the initial position.

As can be seen from Figs. 18 and 19, the variation law of the constraint force/torque of the metamorphic joint before and after the configuration change has changed greatly, and there is a sudden change between the constraint force/torque of the metamorphic joints at the time of configuration change. The sudden change is related to the impact of configuration change.

4.2 The Metamorphic Nipper Swing Mechanism

Taking the metamorphic nipper swing mechanism (Zhang and Sun 2015) as an example, the types and constraints of metamorphic joints based on the kinematic characteristics of metamorphic joints are given. The mechanism has three configurations, which are: the nipper is gradually closed, the nipper is closed, and the nipper is gradually opened during working cycle. Based on that, the nipper gradually closed configuration and the nipper gradually opened configuration are taken as a mechanism in order to achieve the above requirements, as shown in Fig. 20a. In this mechanism, spring is added to kinematic joint G, so that the slider 5 and the component 6 are combined into one component under the constraint of spring, and the nipper is in an open state at this time. The nipper closed configuration is shown in Fig. 20b. In this mechanism, a geometric constraint is added at kinematic joint C, and the upper nipper 4 which combined with the lower nipper 2 to form one component is gradually moved from position b to position a.

Based on the principle of augmented Assur groups, the metamorphic nipper swing mechanism is divided into a fixed-axis rotating active part, an Assur group RPR and an augmented Assur group RP–RR–RR–R, as shown in Fig. 21.

According to geometric and inertia properties of the metamorphic nipper swing mechanism in Table 3, a three-dimensional model is established in SolidWorks, as shown in Fig. 22. The initial distance between slider 5 and H is 172.37 mm, and the initial position of the component 9 is $3\pi / 5$ rad.

Assuming that the active part 9 rotates at a constant speed of 6 r/min (motion period is 10 s), the dynamic simulation is carried out in SolidWorks virtual prototype environment, and the relationship between the driving torque and time of the metamorphic nipper swing mechanism is obtained.

Table 3 Geometric and inertia properties of the metamorphic nipper swing mechanism (SI units)

Parameter	Measurement value	Parameter	Measurement value
L_{AB}	0.082	m_8	0.067
L_{BC}	0.112	m_9	0.04
L_{CE}	0.075	J_1	1.583×10^{-3}
L_{ED}	0.074	J_{2C}	3.51×10^{-4}
L_{CF}	0.075	J_3	3.3×10^{-5}
L_{OP}	0.065	J_{4C}	3.4×10^{-5}
m_1	0.165	J_5	6.6×10^{-6}
m_2	0.098	J_6	2.59×10^{-4}
m_3	0.044	J_8	6.6×10^{-6}
m_4	0.045	J_9	2.5×10^{-5}
m_5	0.067	k	2000
m_6	0.088	c	1000

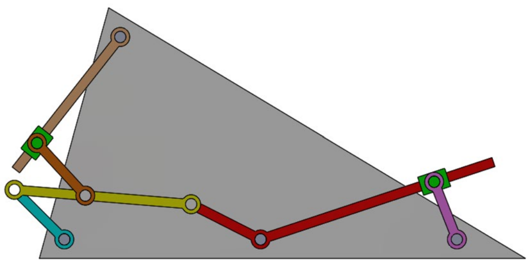

Fig. 22 Three-dimensional graph

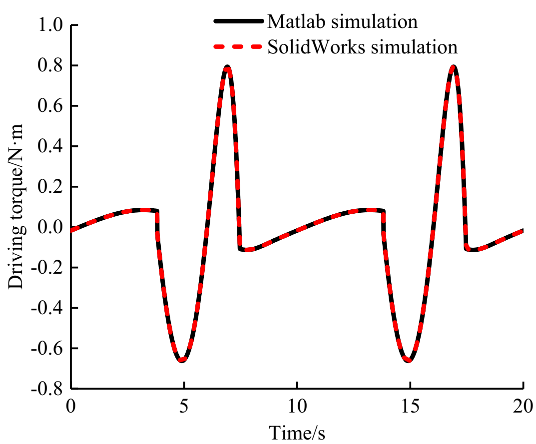

Fig. 23 Driving torque of the metamorphic nipper swing mechanism

When the metamorphic nipper swing mechanism is in gradually closed and gradually opened configurations, the dynamic equations can be obtained by Eqs. (1), (2) and (7). When the mechanism is in closed configuration, the dynamic equations can be obtained by Eqs. (1), (2) and (8). The parameters in Table 3 are substituted into the dynamic equations of the metamorphic nipper swing mechanism, and the numerical iterative algorithm is adopted (the iteration time step is 0.01 s). The relationship between driving torque and time is obtained by using Matlab numerical simulation software. The results are compared with SolidWorks virtual dynamics simulation.

As shown in Fig. 23, the numerical results of driving torque are in good agreement with those of virtual simulation. It verifies the correctness and validity of the Class III augmented Assur groups dynamics model.

5 Conclusions

Based on the constrained metamorphic mechanisms, a simple and straightforward approach to develop a unified dynamics model and a systematic numerical iterative algorithm for solving dynamic equations were presented in this paper, considering the impact of force constraints and/or geometric constraints.

What conclusions can be arrived in this paper are as following,

(1) Presented a simple and straightforward approach to establish a unified dynamics model of constrained metamorphic mechanisms considered force constraints and/or geometric constraints. In this approach, a unified dynamics model of constrained metamorphic mechanisms is composed of dynamics models of active parts, Assur groups and augmented Assur groups, and all of these models are established by N/E equation. In the dynamics model of augmented Assur groups, metamorphic joints have an important influence on augmented Assur groups. By considering the kinematic characteristics of the metamorphic joints, there are non-collision configuration, internal collision configuration and external collision configuration. Meanwhile, the complete configuration dynamics model of augmented Assur groups is established.

(2) Proposed a numerical iterative algorithm for solving the dynamic equations of constrained metamorphic mechanisms based on the theory that velocity and acceleration are same in an extremely brief period. It solves the difficult problem for the dynamic solution of constrained metamorphic mechanisms due to the existence of non-holonomic constraints and strong coupling.

(3) Taking the planar double-folded metamorphic mechanism and the metamorphic nipper swing mechanism as examples, the numerical simulations are finished by Matlab software and SolidWorks software. Simulation results show that the unified dynamics model of constrained metamorphic mechanisms and the numerical iterative algorithm are correct and effective. On the other hand, it shows that impact motion of constrained metamorphic mechanisms exists in the transformation of configuration, and it provides a theoretical basis for the follow-up study of such mechanisms.

Acknowledgements This research was sponsored by the National Natural Science Foundation of China (Nos. 51275352, 51475330), Natural Science Foundation of Tianjin (Nos. 17JCQNJC03900, 18JCQNJC05300) and the Program for Innovative Research Team in University of Tianjin (No. TD13-5037).

Compliance with Ethical Standards

Conflict of interest The authors have declared that no competing interests exist.

Appendix 1

See Table 4.

Table 4 Dynamic analysis of Class II and III Assur group

<table>
<tr><th>Assur group name</th><th colspan="2">Dynamics analysis of Assur group</th></tr>
<tr><td rowspan="3">Class II Assur group</td><td>(1) RRR

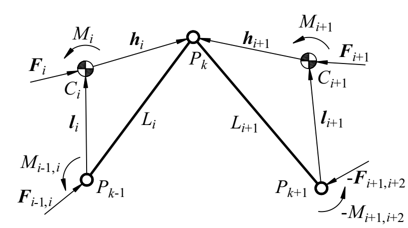
</td><td>(2) RRP

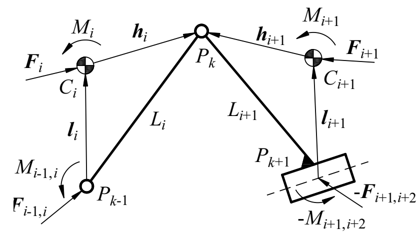
</td></tr>
<tr><td>(3) RPR

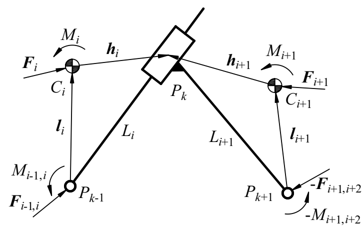
</td><td>(4) PRP

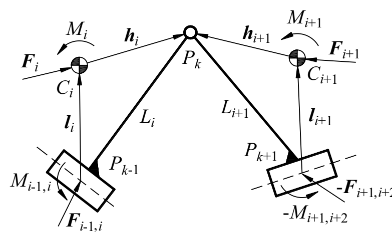
</td></tr>
<tr><td colspan="2">(5) PPR

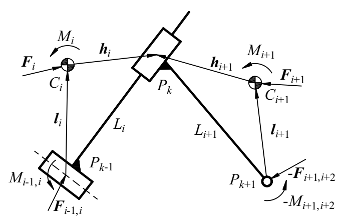
</td></tr>
<tr><td rowspan="2">Class III Assur group</td><td>(1) RR-RR-RR

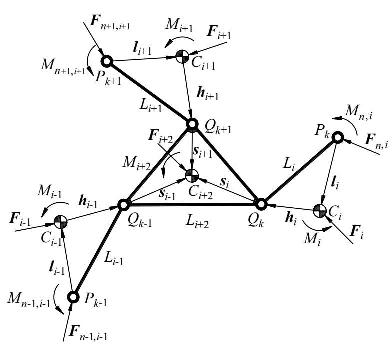
</td><td>(2) RP-RR-RR

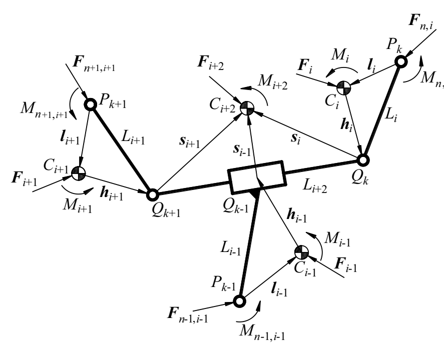
</td></tr>
<tr><td>(3) PR-RP-RR

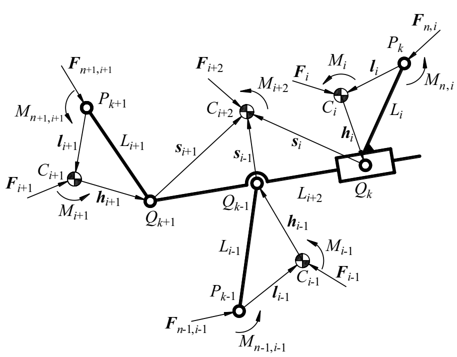
</td><td>(4) RP-PR-RP

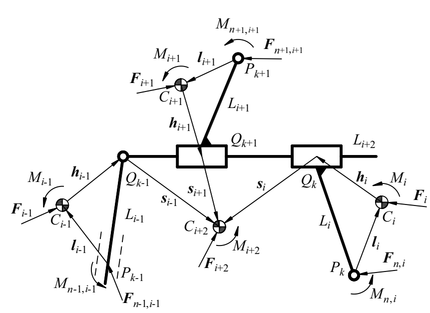
</td></tr>
</table>

Appendix 2

See Table 5.

Table 5 Dynamic analysis of Class II and III augmented Assur group

Augmented Assur group name	Class II and III augmented Assur group	
	Structure diagram	Dynamics analysis of augmented Assur group
Class II augmented Assur group	(1) RRRR 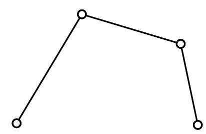	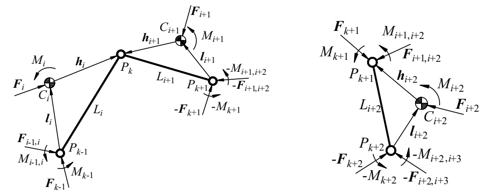
	(2) RRPR 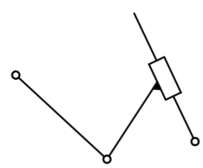	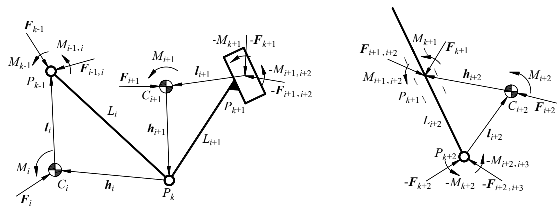
	(3) RPPR 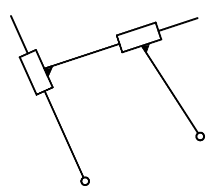	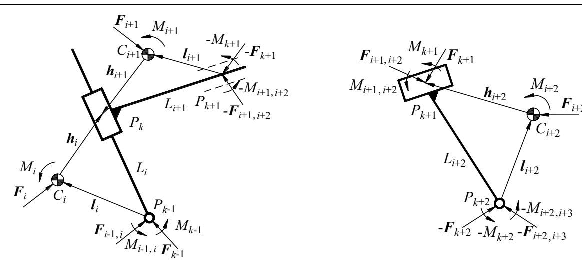
	(4) RRRP 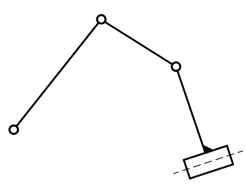	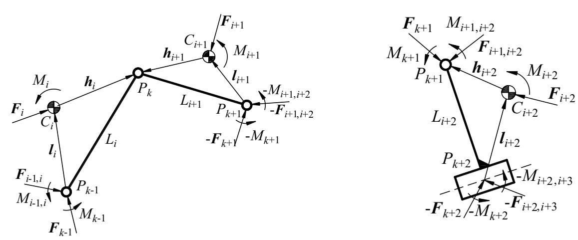
	(5) RRPP 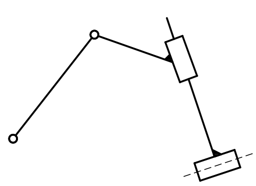	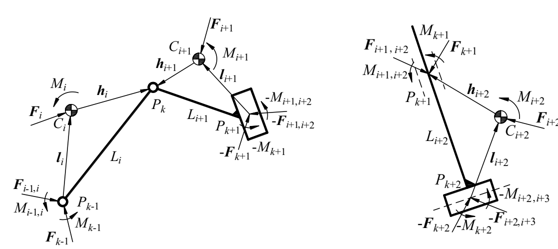
	(6) RPRP 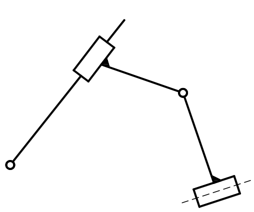	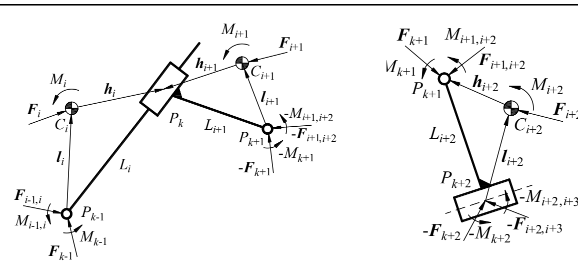

Table 5 (continued)

Augmented Assur group name	Class II and III augmented Assur group	
	Structure diagram	Dynamics analysis of augmented Assur group
Class II augmented Assur group	(7) RPPP 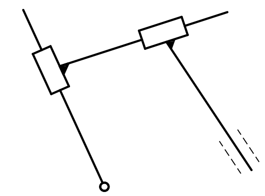	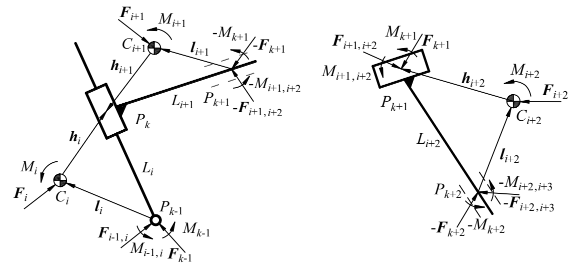
	(8) PRRP 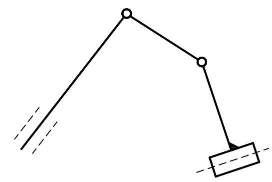	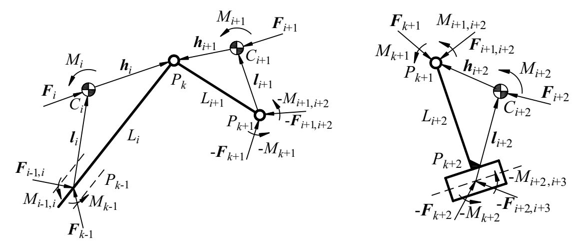
	(9) PRPP 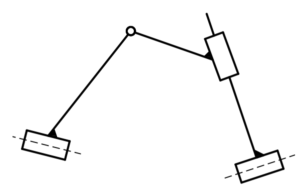	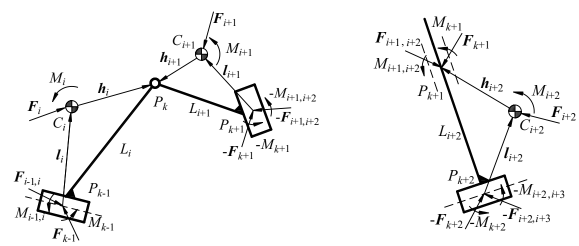
Class III augmented Assur group	(1) RR-RR-RR-R 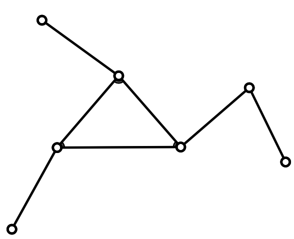	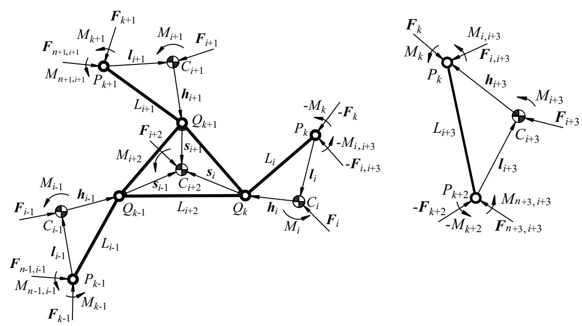
	(2) RR-PR-RR-R 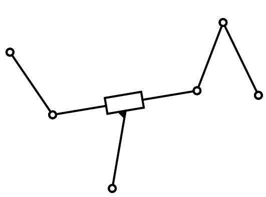	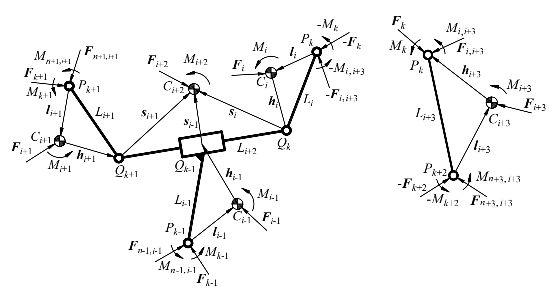

References

Dai JS, Rees JJ (1997) New configuration model of cartons and their operation[R]. Science and Technology Report, PS, Unilever Research 97:0066

Dai JS, Rees JJ (1997) Structure and mobility of cartons in cartoning process[R]. Science and Technology Report, PS, Unilever Research 97:0067

Dai JS, Rees JJ (1997) Theory on kinematic synthesis and motion analysis of cartons[R]. Science and Technology Report, PS, Unilever Research, 97:0184

Dai JS, Rees JJ (1999) Mobility in metamorphic mechanisms of foldable/erectable kinds[J]. J Mech Des 121(3):375–382

Ding X, Yang Y (2010) Reconfiguration theory of mechanism from a traditional artifact[J]. J Mech Des 132(11):114501_1–114501_8

Gan D, Dai JS, Liao Q (2009) Mobility change in two types of metamorphic parallel mechanisms[J]. J Mech Robot 1(4):041007_1–041007_9

Gan D, Dai JS, Liao Q (2010) Constraint analysis on mobility change of a novel metamorphic parallel mechanism[J]. Mech Mach Theory 45(12):1864–1876

Gan D, Dai JS, Dias J et al (2013) Unified kinematics and singularity analysis of a metamorphic parallel mechanism with bifurcated motion[J]. J Mech Robot 5(3):011104_1–011104_11

Gan D, Dai JS, Dias J et al (2016a) Joint force decomposition and variation in unified inverse dynamics analysis of a metamorphic parallel mechanism[J]. Meccanica 51(7):1583–1593

Gan D, Dias J, Seneviratne L (2016b) Unified kinematics and optimal design of a 3rRPS metamorphic parallel mechanism with a reconfigurable revolute joint[J]. Mech Mach Theory 96(2):239–254

Jin G, Zhang Q, Dai JS et al (2003) Dynamic modeling of metamorphic mechanism[J]. Chin J Mech Eng 16(1):94–99

Jin G, Ding X, Zhang Q (2004) Research on configuration-complete dynamics modeling and numerical simulation of metamorphic mechanism[J]. Acta Aeronaut Et Astronaut Sin 25(4):401–405

Katake AB, Mahindrakar AD, Banavar RN (2000) Study of underactuated mechanisms in the presence of holonomic constraints: the constrained Acrobot[C]. In: IEEE international conference on industrial technology. IEEE, vol 2, pp 703–706

Kuo C, Yan H (2007) On the mobility and configuration singularity of mechanisms with variable topologies[J]. J Mech Des 129(6):617–624

Li S, Dai JS (2010) Structure of metamorphic mechanisms based on augmented Assur groups[J]. Chin J Mech Eng 46(13):22–41

Li S, Wang H, Yang Q (2015) Constraint force analysis of metamorphic joints based on the augmented Assur groups[J]. Chin J Mech Eng 28(4):747–755

Li S, Wang H, Meng Q et al (2016) Task-based structure synthesis of source metamorphic mechanisms and constrained forms of metamorphic joints[J]. Mech Mach Theory 96:334–345

Liu C, Yang T (2004) Essence and characteristics of metamorphic mechanisms and their metamorphic ways[C]. In: Proceedings of 11th World congress in mechanism and machine science, Mechanical Engineering Press, Tianjin pp 1285–1288

Parise JJ, Howell LL, Magleby SP (2000) Ortho-planar mechanisms. In: Proceedings of the 26th biennial mechanisms and robotics conference, Baltimore, MD, Paperno. DETC2000/MECH-14193

Valsamos C, Moulianitis V, Aspragathos N (2012) Index based optimal anatomy of a metamorphic manipulator for a given task[J]. Robot Comput Integr Manuf 28(4):517–529

Valsamos C, Moulianitis VC, Synodinos AI et al (2015) Introduction of the high performance area measure for the evaluation of metamorphic manipulator anatomies[J]. Mech Mach Theory 86(86):88–107

Wang D, Dai JS (2007) Theoretical foundation of metamorphic mechanisms and their synthesis[J]. Chin J Mech Eng 43(8):32–42

Wang R, Chen H, Dai J (2017) Dynamic stability study of a novel controllable metamorphic palletizing robot mechanism[J]. Chin J Mech Eng 53(13):39–47

Xiong P, Lai X, Wu M (2015) Position and attitude control for a class of planar underactuated mechanical system with second order non-holonomic constraints[J]. J Southeast Univ 45(4):690–695

Xu K, Li L, Bai S et al (2017) Design and analysis of a metamorphic mechanism cell for multistage orderly deployable/retractable mechanism[J]. Mech Mach Theory 111:85–98

Yan H, Kuo C (2006) Topological representations and characteristics of variable kinematic joints[J]. J Mech Des 128(2):384–391

Zhang W, Ding X (2012) A method for configuration representation of metamorphic mechanisms with information of component variation[M]. In: Advances in reconfigurable mechanisms and robots I. Springer, London vol 8, pp 1949–1956

Zhang H, Sun Z (2015) Improvement on the operation rule of metamorphic mechanism generalized adjacent matrix[J]. J Donghua Univ 41(6):802–807

Zhang K, Dai JS, Fang Y (2010) Topology and constraint analysis of phase change in the metamorphic chain and its evolved mechanism[J]. J Mech Des 132(12):121001_1–121001_11

Zhang Z, Sun J, Wang Z et al (2016) Quaternion method for the kinematics analysis of parallel metamorphic mechanisms[M]. Advances in reconfigurable mechanisms and robots II. Springer, Berlin